Spatiotemporal Acoustic Vortex Beams with Transverse Orbital Angular Momentum

Hao Ge,[1] Shuai Liu,[1] Xiang-Yuan Xu,[1] Zi-Wei Long,[1] Yuan Tian,[1]
Xiao-Ping Liu,[2,*] Ming-Hui Lu,[1,3,4,†] and Yan-Feng Chen[1,4,‡]
[1]National Laboratory of Solid State Microstructures & Department of Materials Science and Engineering, Nanjing University, Nanjing, Jiangsu 210093, China
[2]School of Physical Science and Technology, ShanghaiTech University, Shanghai 201210, China
[3]Jiangsu Key Laboratory of Artificial Functional Materials, Nanjing University, Nanjing, Jiangsu 210093, China
[4]Collaborative Innovation Center of Advanced Microstructures, Nanjing University, Nanjing 210093, China

(Received 10 January 2023; accepted 16 May 2023; published 7 July 2023)

Recently, the discovery of optical spatiotemporal (ST) vortex beams with transverse orbital angular momentum (OAM) has attracted increasing attention and is expected to extend the research scope and open new opportunities for practical applications of OAM states. The ST vortex beams are also applicable to other physical fields that involve wave phenomena, and here we develop the ST vortex concept in the field of acoustics and report the generation of Bessel-type ST acoustic vortex beams. The ST vortex beams are fully characterized using the scalar approach for the pressure field and the vector approach for the velocity field. We further investigate the transverse spreading effect and construct ST vortex beams with an ellipse-shaped spectrum to reduce the spreading effect. We also experimentally demonstrated the orthogonality relations between ST vortex beams with different charges. Our study successfully demonstrates the versatility of the acoustic system for exploring and discovering spatiotemporally structured waves, inspiring further investigation of exotic wave physics.

DOI: 10.1103/PhysRevLett.131.014001

Introduction.—Exploiting the spin and orbital angular momentum (AM) opens up new dimensions for manipulating waves [1–8] and their interaction with matters [9]. It has enabled unique applications in areas such as communications, metrology, tweezers, and nanophotonics. Generally, the spin and orbital AM carried by waves are longitudinal and along the wave propagation direction. However, in some exceptional cases that involve strong focusing or structured fields, the AM can be transverse [10]. The electromagnetic fields in spatially confined evanescent fields can carry a transverse spin angular momentum (SAM) [11,12]. Very recently, a new exotic class of spatiotemporal (ST) vortex beams has been discovered in optics [13–27], which carries an intrinsic orbital angular momentum (OAM) transverse to the beam propagation direction.

The vortex beams are widely studied in various fields, resulting in many important applications [8]. The conventional vortex beams carrying longitudinal OAM have a three-dimensional helical wavefront arising from the spiral phase profile in the spatial domain. The helical wavefront can produce a measurable torque on the object. The vortex beams are characterized by the integer topological charge, which indicates the number of wavefront twists in one wavelength along the propagation direction. The vortex beams with different topological charges provide theoretically infinite orthogonal channels, enabling high-capacity information transmission. This unique wave field was recently discovered in the spatial-temporal domain and categorized as ST vortex beams. Unlike the conventional vortex beams, the ST vortex beams can exist in the two-dimensional (2D) space ($x-z$ plane, or the $x-t$ plane considering z direction wave propagation), as shown in Fig. 1(a). The vortex structure carries an OAM perpendicular to the propagation direction, i.e., y direction in the figure, resulting from the spiral phase profile in the spatial-temporal domain. The ST vortex beams with transverse OAM were recently generated experimentally in optics, and the diffraction properties and second-harmonic generation process have also been studied [15–27]. The transverse OAM could provide additional degrees of freedom and extend the research and application scopes of OAM states.

Acoustics is an utterly important and popular platform for researching cutting-edge wave physics and its immediate applications. For instance, acoustic vortex beams can be readily generated by active phased arrays or passive acoustic metasurfaces [28–34]. They can find applications in particle manipulation [35,36], asymmetric propagation [37], and high-speed acoustic communication [38]. The instantaneous spatial and temporal acoustic field profiles can be directly characterized via acoustic sensors. However, the OAM carried by conventional acoustic vortex beams are restricted to be longitudinal, and the acoustic vortex beams are also monochromatic in most cases. Here, we develop the ST vortex concept in the field of acoustics and report a comprehensive investigation of Bessel-type ST

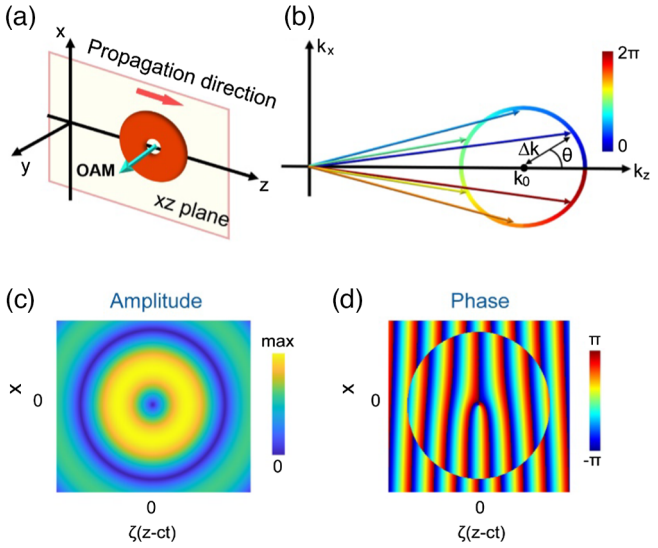

FIG. 1. (a) Schematic of a representative ST vortex beam. The ST vortex beam can exist in the 2D plane and carry a transverse OAM. (b) The plane-wave angular spatial frequency spectrum for the Bessel-type ST vortex beam. A spiral phase is applied over the circle. The Bessel-type ST vortex beam is constructed by a superposition of the plane waves with their corresponding angular spatial frequency and initial phase on the circle. (c), (d) Theoretically calculated amplitude (c) and phase (d) distribution of the ST vortex beam with $l = 1$.

acoustic vortex beams. The polychromatic ST acoustic vortex beams are fully characterized with a complete description of acoustic waves involving the four-component vector $(p, \mathbf{v})$, conveying the importance of the vectorial velocity nature of acoustic waves [39–43]. The transverse spreading effect of the ST vortex beams is further investigated, and the construction of ST vortex beams with an ellipse shape is then proposed to reduce the spreading effect. In addition, the orthogonality relations between ST vortex beams with different charges are demonstrated. The realization of the acoustic ST vortex beams will open new opportunities for practical applications of acoustic OAM. Our work also paves the promising way for further studies, such as generating arbitrarily oriented acoustic OAM states [44] and fractional OAM states [45]. ST vortex beams also represent a compelling example of space-time wave packets, which have yet to be extensively explored in the realm of acoustics due to the predominantly monochromatic nature of acoustic waves.

Bessel-type spatiotemporal acoustic vortex beams.—We consider acoustic waves in a 2D acoustic waveguide, and the acoustic pressure field p is governed by the equation

$$\nabla^2 p - \frac{1}{c^2}\frac{\partial^2 p}{\partial t^2} = 0, \tag{1}$$

where c is the speed of the acoustic wave. The acoustic plane wave mode is described as $p = p_0 e^{i(\boldsymbol{kr}-\omega t)}$, and the wave vector $|\boldsymbol{k}| = \omega/c$. The Bessel-type ST vortex beams are polychromatic waves constructed by a superposition of plane waves with wave vectors distributed on a circle in the angular spatial frequency domain [Fig. 1(b)] and a spiral phase $e^{il\theta}$ for that circle of wave vectors. The resulting real-space acoustic pressure wave function can then be expressed as the sum of these plane waves [18]:

$$p(x, z, t) \propto \int_0^{2\pi} e^{i[k_0 z + \Delta k \cos\theta z + \Delta k \sin\theta x + l\theta - \omega(\theta) t]} d\theta, \tag{2}$$

where Δk is the circle radius, θ is the azimuthal angle, l is the topological charge, $(k_0, 0)$ is the location of the circle center in the angular spatial frequency space, and $\omega(\theta) = c\sqrt{k_0^2 + \Delta k^2 + 2k_0 \Delta k \cos\theta}$. For $\Delta k \ll k_0$, the ST vortex beams can be considered near-paraxial and $\omega(\theta) \simeq c(k_0 + \Delta k \cos\theta)$. Under this approximation, Eq. (1) can be simplified as follows:

$$p(x, z, t) \propto J_l(\Delta k r) e^{i(k_0 \zeta + l\varphi)}, \tag{3}$$

where J_l is the l th order of the Bessel function of the first kind, $\zeta = z - ct = r\cos\varphi$, (r, φ) is the polar coordinate in the (ζ, x) plane. The term $e^{il\varphi}$ corresponds to the spiral phase structure in the spatial-temporal domain with topological charge number l. The distributions of $|p|$ and the corresponding phase angle $\mathrm{Arg}(p)$ with $l = 1$ are shown in Figs. 1(c) and 1(d), respectively. There is a singularity of zero intensity at the center, and the phase distribution shows an edge dislocation, which is produced by the spiral phase structure. The edge phase dislocation has also been observed in water waves, which is an analog of Aharonov-Bohm effect [46,47]. The surface water waves are scattered by an irrotational vortex, and a geometric phase shift is picked up in the scattering process, which leads to the nontrivial phase structure.

The schematic of our experimental setup is shown in Fig. 2(a). The experiment is conducted in a 2D acoustic waveguide with a height of 2 cm (see details in Supplemental Material [48]). Sound-absorbing foams are placed at the boundaries of the waveguide to avoid reflections. We choose 10 modes with their spatial frequencies distributed equally on the circle in Fig. 1(b), with $k_0 = 119\ (\mathrm{rad/m})$ and $\Delta k = 0.15 k_0$, and the corresponding acoustic frequency range is 5525–7475 Hz. According to Eq. (2), Δk determines the size of the ST vortex; in this case, it is ~50 cm in the spatial domain and ~2 ms in the time domain. These 10 modes with equal intensities but different frequencies, phases, and propagation directions are generated by an acoustic phased array controlled by a multichannel sound card. The acoustic phased array consists of 20 speakers with a spacing of 3.3 cm. The ST acoustic vortex beams can be characterized either in the $x - z$ plane by a time snapshot or the $x - t$ spatial-temporal domain at a fixed z position. Here, we employ the later

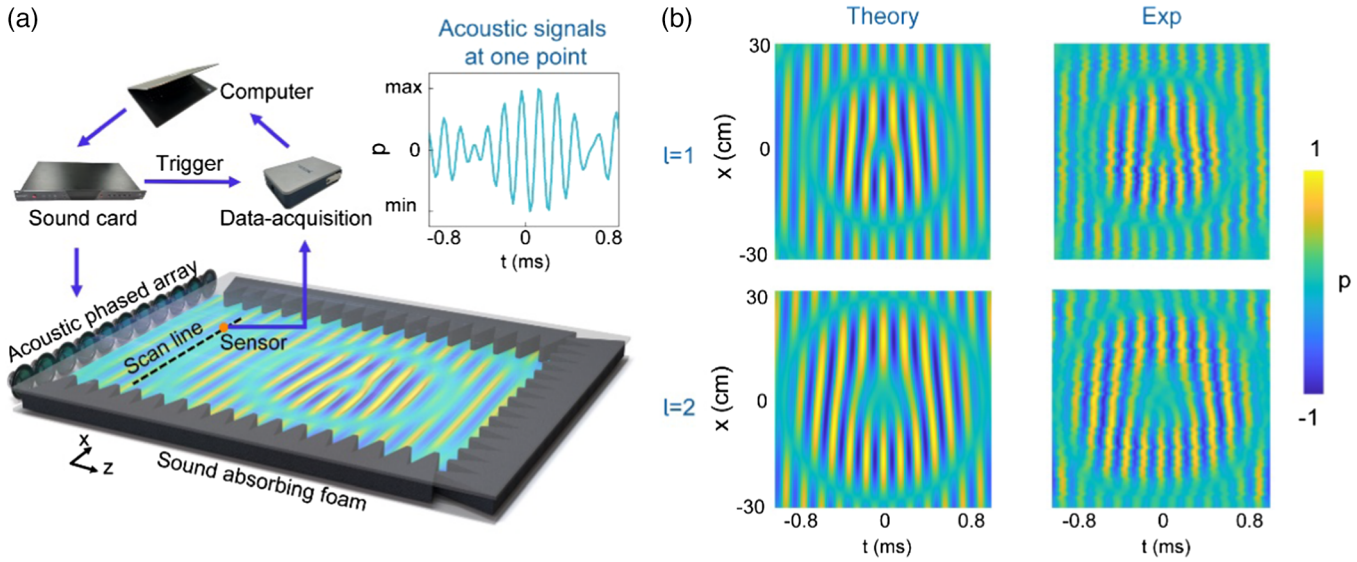

FIG. 2. (a) Schematic of our experimental setup. The ST vortex beam is generated by an acoustic phased array and measured along a scan line. A separate pulse signal from the sound card synchronously triggers each recording. The inset shows a time sequence of acoustic signals acquired at one point. Theoretically calculated and experimentally measured pressure fields are shown in (b) for the $l = 1$ vortex and the $l = 2$ vortex, respectively, which show clear evidence of the signature edge phase dislocation.

characterization method by recording a time sequence of acoustic signals at each point along a scan line (here, $z = 0$), as shown in Fig. 2(a). A separate pulse signal from the sound card synchronously triggers each recording. The inset shows the recorded acoustic signals at one point.

Figure 2(b) presents the theoretically calculated [via Eq. (1)] and experimentally measured acoustic ST vortex beam with two topological charges, $l = 1$ and $l = 2$, respectively. The time $t = 0$ corresponds to the moment when the center location of the vortex beam reaches $z = 0$. The measured normalized pressure fields, $p(x, z = 0, t)$, agree remarkably well with the theoretical results. In both cases, there is clear evidence of the signature edge phase dislocation, which is tied to the topological charge of the vortex beam. The vortex beams with charge l have an azimuthal phase dependence $e^{il\varphi}$ in the spatial-temporal domain. The transverse OAM carried by the vortex is determined by the azimuthal phase gradient of the field, and is linearly proportional to the topological charge l. It has been reported that the transverse OAM also depends on the eccentricity of the intensity distribution and dispersion of the medium [18,19]. This study demonstrates that different ST vortex beams can be readily generated in acoustics, allowing for rapid deployment of a study platform for the rich physics of these exotic beams.

Vector velocity field.—Prior studies on acoustic OAM mainly focus on the pressure field p, which is a scalar representation. However, acoustic waves can have a full vectorial representation, characterized by the vector velocity field $\mathbf{v}$ that is related to the pressure field as $i\omega\rho\mathbf{v} = \nabla p$ for monochromatic waves. This vectorial field leads to much more abundant physics of the acoustic waves beyond their scalar representation. The canonical momentum density $\mathbf{p}$, determining the OAM of acoustic fields, is given by $\mathbf{p} = (1/4\omega)\mathrm{Im}[\beta p^* \nabla p + \rho \mathbf{v}^* \cdot (\nabla)\mathbf{v}]$ [40], where β is the compressibility of the medium and ρ is the mass density. This relationship suggests that the velocity field is a fundamental physic parameter contributing to the OAM of acoustic fields.

The distribution of the vector velocity field of the ST vortex beam could be different from the scalar pressure field. As shown in Fig. 3(a), the green arrows denote the direction of the velocity vector of each plane wave component, which is parallel to the plane wave's wave vector. For $\Delta k \ll k_0$, the z component of the velocity vector $v_z \simeq |\mathbf{v}|$, and the x component $v_x \simeq |\mathbf{v}|(\Delta k \sin\theta/k_0)$. The velocity field of the ST vortex beam can be expressed as [18]

$$v_z \propto J_l(\Delta k r) e^{i(k_0\zeta + l\varphi)}$$
$$v_x \propto \frac{i\Delta k}{2k_0} e^{ik_0\zeta}[e^{i(l-1)\varphi} J_{l-1}(\Delta k r) + e^{i(l+1)\varphi} J_{l+1}(\Delta k r)]. \quad (4)$$

In our experiment, the velocity field is directly measured via a 2D acoustic vector sensor, and the two components v_x and v_z are acquired simultaneously (see details in Supplemental Material [48]). As an illustration, we set $k_0 = 59.5\ (\mathrm{rad/m})$ and $\Delta k = 0.25k_0$, corresponding to a frequency range of 2437–4062 Hz. The theoretical and experimental results of the velocity field are shown in Figs. 3(b), 3(c). The result of the v_z component is similar to the pressure field discussed above. The v_x component is described by Bessel functions of the first kind of orders

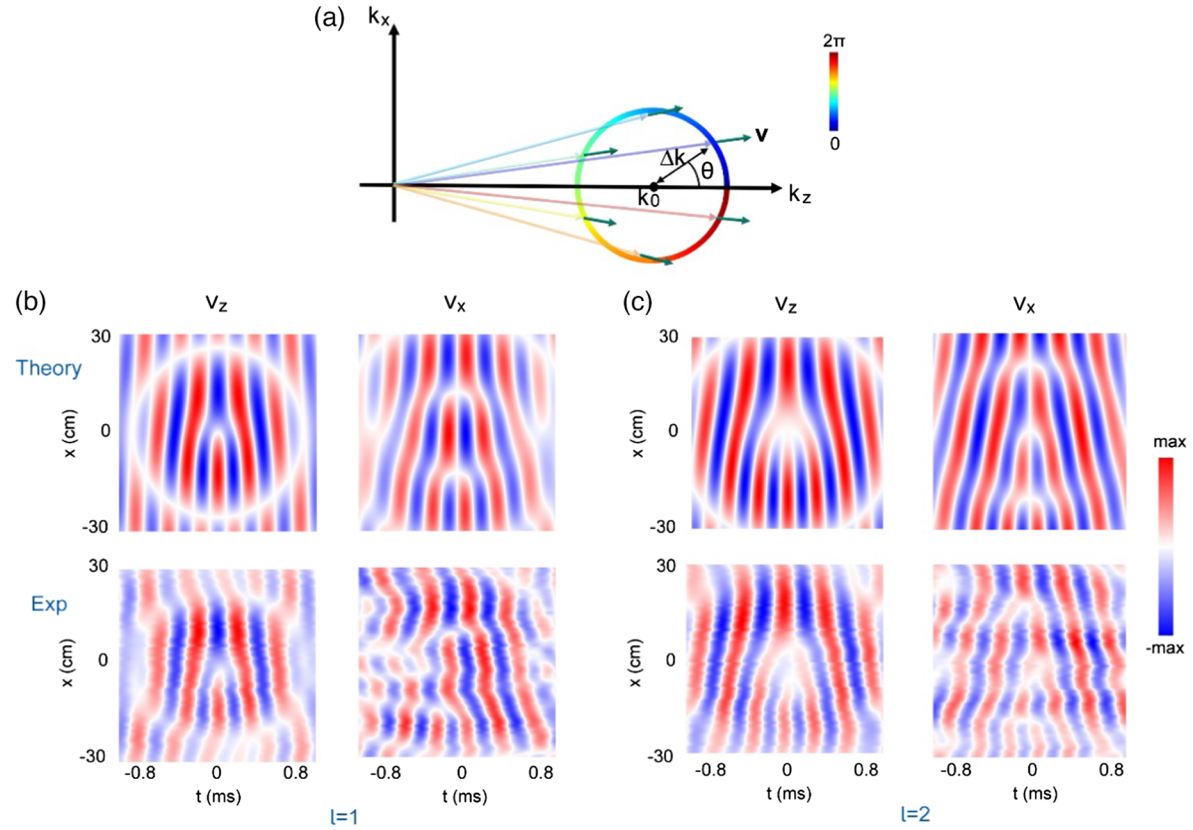

FIG. 3. (a) The plane-wave spectrum for the Bessel-type ST vortex beams. The green arrows denote the direction of the velocity vector, which is parallel to the wave vector of the plane wave component. Theoretically calculated and experimentally measured velocity fields are shown in (b) for the $l = 1$ vortex and (c) for the $l = 2$ vortex.

$l \pm 1$, and multiple dislocations exist in the field distribution. When $l = 1$, the velocity field exhibits a nonzero field intensity at the center, which is the signature of the spin-orbit interaction effect [18]. The vortex beam is constructed by a superposition of plane waves, and the interference of plane waves with different propagation directions can generate a nonzero transverse acoustic SAM density. The acoustic SAM is associated with the elliptically polarized profile of acoustic velocity fields, while the acoustic OAM depends on the azimuthal phase gradient of fields. The spin-orbit interaction occurs between the transverse OAM and SAM of the ST vortex beam [18,40].

Transverse spreading effect.—The propagation of acoustic ST vortex beams can lead to shape distortions, owning to the transverse spatial spreading effect along the x direction. This is a fundamental attribute of spatiotemporal vortex beams [19]. In order to mitigate the shape distortions, we demonstrate that compressing the circular spectrum along the k_x axis helps to suppress the transverse spreading effect. For example, as shown in Fig. 4(a), the above circular spectrum transforms into an elliptical spectrum with the ratio of semiaxes $g = 2$. The corresponding vortex beam in real space is stretched along the x direction [Fig. 4(b)]. The manipulation of the spectrum increases the acoustic equivalent Rayleigh range and reduces the spreading of the acoustic structure along the x direction.

Using a similar experimental technique described in the previous section, we generate the ST vortex beam with the compressed spectrum and measure its pressure field along the $z = 0$ scan line. Meanwhile, Eq. (1) is modified to study the transverse spreading effect by replacing z with $z + 5ct_R$, with $ct_R = k_0/\Delta k^2$, where t_R is the corresponding characteristic timescale. As a result, in Eq. (2), ζ is replaced with $\zeta = z + 5ct_R - ct$, and the time $t = 5t_R$ corresponds to the moment when the center of the ST vortex beam reaches $z = 0$. Figure 4(c) present the theoretical and experimental results of the transverse spreading effect for the ST vortex beam with $l = 1$, which show that the vortex beam splits into offset lobes at $t = 5t_R$. In comparison, the shape of the stretched vortex beam remains almost undistorted at $t = 5t_R$ [Fig. 4(d)], which demonstrates that the transverse spreading effect is greatly suppressed.

Orthogonality relations between ST vortex beams.—A critical application of OAM modes is high-capacity communication that exploits mode multiplexing enabled by the orthogonality between OAM modes. The conventional OAM multiplexing technique is based on the orthogonality

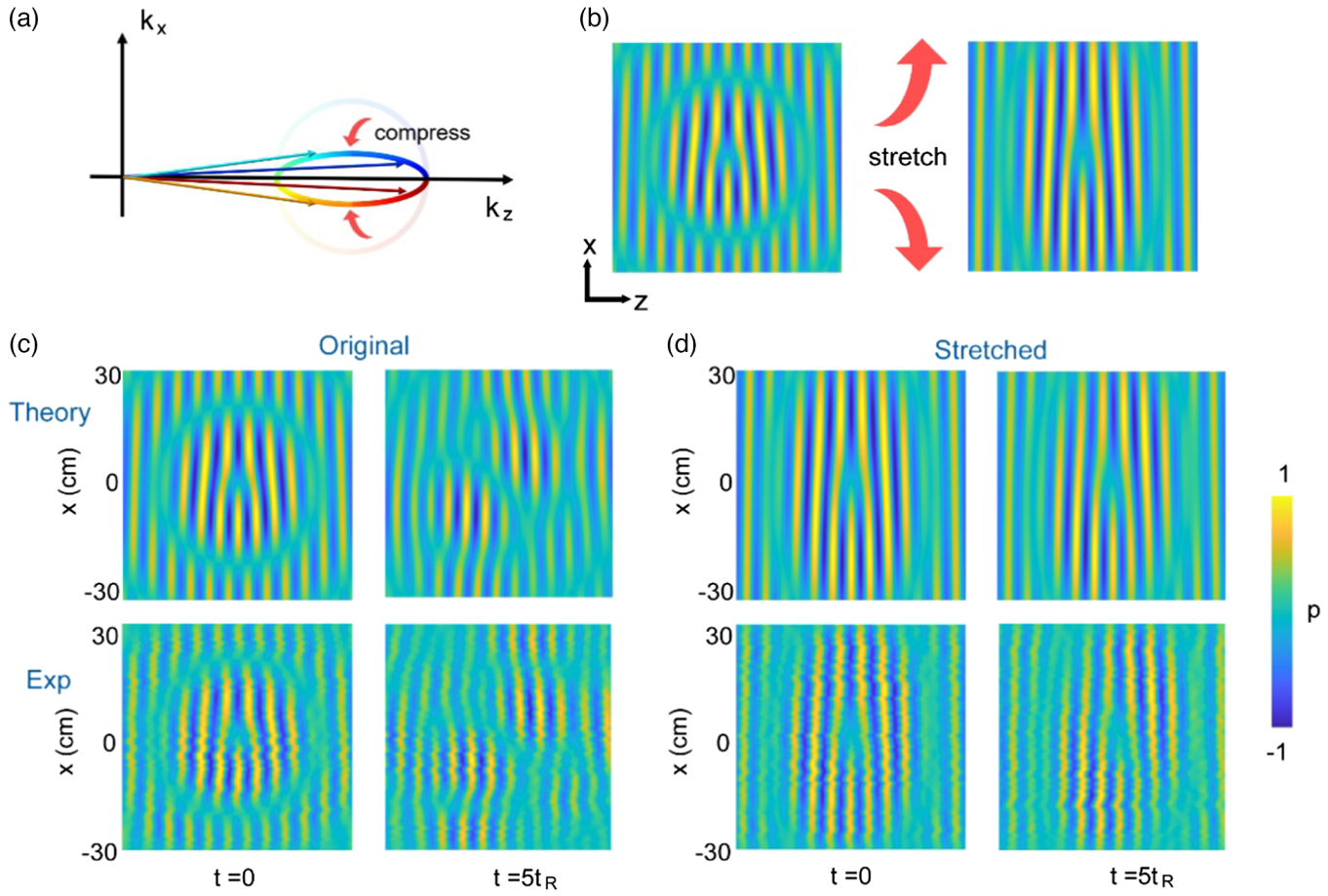

FIG. 4. (a) The plane-wave spectrum for the deformed ST vortex beam. The circular spectrum is compressed along the k_x axis. (b) The ST vortex beam is stretched along the x axis in real space. (c) Theoretically calculated and experimentally measured results of the transverse spreading effect for the original vortex beam. The vortex beam splits into two parts at $t = 5t_R$. (d) Theoretically calculated and experimentally measured results for the deformed vortex beam. The vortex remains almost undistorted at $t = 5t_R$.

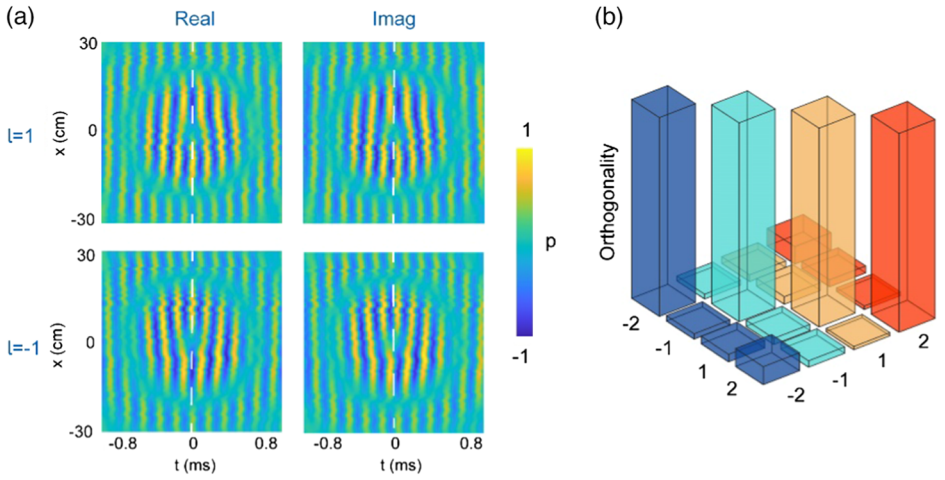

FIG. 5. (a) The real and imaginary parts of the pressure field with $l = 1$ and $l = -1$. The imaginary part is obtained by applying a Hilbert transform to the measured real part. (b) Orthogonality relations between the ST vortex beams with charges -2 to $+2$ are obtained by the inner product of the two corresponding complex pressure fields in the spatial-temporal domain.

in the spatial degree of freedom. Here, we demonstrate that the orthogonality relation still holds for the ST vortex with a spatial-temporal degree of freedom. The orthogonality relation is obtained by the inner product of the two corresponding pressure fields in the spatial-temporal domain:

$$I_{jl} = \frac{\int p_j^* p_l dxdt}{\int p_l^* p_l dxdt}, \tag{5}$$

where $p_l(x,t)$ is the complex pressure field of the ST vortex with charge l. In our experiment, only the real part of the pressure field is directly measured, and the corresponding imaginary part is obtained via a Hilbert transform (see details in Supplemental Material [48]). As an illustration, the complex pressure fields for charge $l = 1$ and $l = -1$ are shown in Fig. 5(a). The measured orthogonality relation between the ST vortex beams with charges from -2 to $+2$ is shown in Fig. 5(b), where only the diagonal element is significant. This finding confirms the low cross-talk nature between different modes.

Conclusion.—In summary, we report the generation of ST acoustic vortex beams, which contain an edge phase dislocation and carry an intrinsic transverse OAM. The vortex beams are characterized in the spatiotemporal domain using the scalar pressure field and the vector velocity field. We also observe the transverse spreading effect and construct ST vortex beams with an ellipse-shaped spectrum to reduce the spreading. The transverse OAM provides extra degrees of freedom for manipulating acoustic waves, which could find applications in acoustic communication and tweezers. The insertion of multiple ST vortex pulses with different charges into a single pulse represents a promising strategy for improving data transmission rates. Leveraging the OAM multiplexing technique in underwater acoustic communication [38] is particularly advantageous given the limitations of optical communication resulting from strong scattering and absorption. The construction of ST vortex beams in 2D space enables their use in planar 2D systems, as well as facilitating in-plane and instantaneous acoustic manipulation of small objects. This work also prompts an excellent platform for further in-depth studies and exploring the intriguing wave physics, such as spin-orbit coupling effects [5] and dynamic properties [49,51,52] of ST vortex beams. This kind of spatiotemporally structured waves have yet to be studied in acoustics due to the monochromatic nature of acoustic waves in most cases. Our work would inspire the further investigation of other spatiotemporally structured acoustic waves, such as flying-focus wave packets and toroidal pulses, or even the discoveries of whole new classes of exotic waves [53–55].

The work is jointly supported by the National Key R&D Program of China (Grants No. 2021YFB3801801 and No. 2018YFA0306200), and the National Natural Science Foundation of China (Grants No. 11890702, No. 51721001, No. 51732006, and No. 52203358). We also acknowledge the support of the Natural Science Foundation of Jiangsu Province. We thank Prof. Shuang Zhang for helpful discussions.

G. H. and L. S. have contributed equally to this work.

*Corresponding author.
liuxp1@shanghaitech.edu.cn
†Corresponding author.
luminghui@nju.edu.cn
‡Corresponding author.
yfchen@nju.edu.cn

[1] L. Allen, M. W. Beijersbergen, R. J. C. Spreeuw, and J. P. Woerdman, Orbital angular momentum of light and the transformation of Laguerre-Gaussian laser modes, Phys. Rev. A **45**, 8185 (1992).
[2] G. Molina-Terriza, J. P. Torres, and L. Torner, Twisted photons, Nat. Phys. **3**, 305 (2007).
[3] S. Franke-Arnold, L. Allen, and M. Padgett, Advances in optical angular momentum, Laser Photonics Rev. **2**, 299 (2008).
[4] N. Shitrit, I. Yulevich, E. Maguid, D. Ozeri, D. Veksler, V. Kleiner, and E. Hasman, Spin-optical metamaterial route to spin-controlled photonics, Science **340**, 724 (2013).
[5] K. Y. Bliokh, F. J. Rodríguez-Fortuño, F. Nori, and A. V. Zayats, Spin-orbit interactions of light, Nat. Photonics **9**, 796 (2015).
[6] P. Lodahl, S. Mahmoodian, S. Stobbe, A. Rauschenbeutel, P. Schneeweiss, J. Volz, H. Pichler, and P. Zoller, Chiral quantum optics, Nature (London) **541**, 473 (2017).
[7] J. Chen, C. Wan, and Q. Zhan, Engineering photonic angular momentum with structured light: A review, Adv. Opt. Photonics **3**, 1 (2021).
[8] Y. Shen, X. Wang, Z. Xie, C. Min, X. Fu, Q. Liu, M. Gong, and X. Yuan, Optical vortices 30 years on: OAM manipulation from topological charge to multiple singularities, Light Sci. Appl. **8**, 90 (2019).
[9] G. F. Quinteiro Rosen, P. I. Tamborenea, and T. Kuhn, Interplay between optical vortices and condensed matter, Rev. Mod. Phys. **94**, 035003 (2022).
[10] K. Y. Bliokh and F. Nori, Transverse and longitudinal angular momenta of light, Phys. Rep. **592**, 1 (2015).
[11] A. Aiello, P. Banzer, M. Neugebauer, and G. Leuchs, From transverse angular momentum to photonic wheels, Nat. Photonics **9**, 789 (2015).
[12] K. Y. Bliokh, A. Y. Bekshaev, and F. Nori, Extraordinary momentum and spin in evanescent waves, Nat. Commun. **5**, 3300 (2014).
[13] A. P. Sukhorukov and V. V. Yangirova, Spatio-temporal vortices: Properties, generation and recording, Proc. SPIE Int. Soc. Opt. Eng. **5949**, 594906 (2005).
[14] K. Y. Bliokh and F. Nori, Spatiotemporal vortex beams and angular momentum, Phys. Rev. A **86**, 033824 (2012).
[15] N. Jhajj, I. Larkin, E. W. Rosenthal, S. Zahedpour, J. K. Wahlstrand, and H. M. Milchberg, Spatiotemporal Optical Vortices, Phys. Rev. X **6**, 031037 (2016).

[16] S. W. Hancock, S. Zahedpour, A. Goffin, and H. M. Milchberg, Free-space propagation of spatiotemporal optical vortices, Optica **6**, 1547 (2019).
[17] A. Chong, C. Wan, J. Chen, and Q. Zhan, Generation of spatiotemporal optical vortices with controllable transverse orbital angular momentum, Nat. Photonics **14**, 350 (2020).
[18] K. Y. Bliokh, Spatiotemporal Vortex Pulses: Angular Momenta and Spin-Orbit Interaction, Phys. Rev. Lett. **126**, 243601 (2021).
[19] S. W. Hancock, S. Zahedpour, and H. M. Milchberg, Mode Structure and Orbital Angular Momentum of Spatiotemporal Optical Vortex Pulses, Phys. Rev. Lett. **127**, 193901 (2021).
[20] J. Huang, J. Zhang, T. Zhu, and Z. Ruan, Spatiotemporal differentiators generating optical vortices with transverse orbital angular momentum and detecting sharp change of pulse envelope, Laser Photonics Rev. **16**, 2100357 (2022).
[21] Y. Fang, S. Lu, and Y. Liu, Controlling Photon Transverse Orbital Angular Momentum in High Harmonic Generation, Phys. Rev. Lett. **127**, 273901 (2021).
[22] S. W. Hancock, S. Zahedpour, and H. M. Milchberg, Second-harmonic generation of spatiotemporal optical vortices and conservation of orbital angular momentum, Optica **8**, 594 (2021).
[23] H. Wang, C. Guo, W. Jin, A. Y. Song, and S. Fan, Engineering arbitrarily oriented spatiotemporal optical vortices using transmission nodal lines, Optica **8**, 966 (2021).
[24] G. Gui, N. J. Brooks, H. C. Kapteyn, M. M. Murnane, and C.-T. Liao, Second-harmonic generation and the conservation of spatiotemporal orbital angular momentum of light, Nat. Photonics **15**, 608 (2021).
[25] J. Chen, C. Wan, A. Chong, and Q. Zhan, Experimental demonstration of cylindrical vector spatiotemporal optical vortex, Nanophotonics **10**, 4489 (2021).
[26] W. Chen, W. Zhang, Y. Liu, F.-C. Meng, J. M. Dudley, and Y.-Q. Lu, Time diffraction-free transverse orbital angular momentum beams, Nat. Commun. **13**, 4021 (2022).
[27] Q. Cao, J. Chen, K. Lu, C. Wan, A. Chong, and Q. Zhan, Non-spreading Bessel spatiotemporal optical vortices, Sci. Bull. **67**, 133 (2022).
[28] B. T. Hefner and P. L. Marston, An acoustical helicoidal wave transducer with applications for the alignment of ultrasonic and underwater systems, J. Acoust. Soc. Am. **106**, 3313 (1999).
[29] J. Lekner, Acoustic beams with angular momentum, J. Acoust. Soc. Am. **120**, 3475 (2006).
[30] C. E. M. Demore, Z. Yang, A. Volovick, S. Cochran, M. P. MacDonald, and G. C. Spalding, Mechanical Evidence of the Orbital Angular Momentum to Energy Ratio of Vortex Beams, Phys. Rev. Lett. **108**, 194301 (2012).
[31] X. Jiang, Y. Li, B. Liang, J.-c. Cheng, and L. Zhang, Convert Acoustic Resonances to Orbital Angular Momentum, Phys. Rev. Lett. **117**, 034301 (2016).
[32] X. Jiang, J. Zhao, S.-l. Liu, B. Liang, X.-y. Zou, J. Yang, C.-W. Qiu, and J.-c. Cheng, Broadband and stable acoustic vortex emitter with multi-arm coiling slits, Appl. Phys. Lett. **108**, 203501 (2016).
[33] N. Jiménez, R. Picó, V. Sánchez-Morcillo, V. Romero-García, L. M. García-Raffi, and K. Staliunas, Formation of high-order acoustic Bessel beams by spiral diffraction gratings, Phys. Rev. E **94**, 053004 (2016).
[34] B. Assouar, B. Liang, Y. Wu, Y. Li, J.-C. Cheng, and Y. Jing, Acoustic metasurfaces, Nat. Rev. Mater. **3**, 460 (2018).
[35] K. Volke-Sepúlveda, A. O. Santillán, and R. R. Boullosa, Transfer of Angular Momentum to Matter from Acoustical Vortices in Free Space, Phys. Rev. Lett. **100**, 024302 (2008).
[36] A. Anhäuser, R. Wunenburger, and E. Brasselet, Acoustic Rotational Manipulation Using Orbital Angular Momentum Transfer, Phys. Rev. Lett. **109**, 034301 (2012).
[37] Y. Fu, Y. Tian, X. Li, S. Yang, Y. Liu, Y. Xu, and M. Lu, Asymmetric Generation of Acoustic Vortex Using Dual-Layer Metasurfaces, Phys. Rev. Lett. **128**, 104501 (2022).
[38] C. Shi, M. Dubois, Y. Wang, and X. Zhang, High-speed acoustic communication by multiplexing orbital angular momentum, Proc. Natl. Acad. Sci. U.S.A. **114**, 7250 (2017).
[39] C. Shi, R. Zhao, Y. Long, S. Yang, Y. Wang, H. Chen, J. Ren, and X. Zhang, Observation of acoustic spin, Natl. Sci. Rev. **6**, 707 (2019).
[40] K. Y. Bliokh and F. Nori, Spin and orbital angular momenta of acoustic beams, Phys. Rev. B **99**, 174310 (2019).
[41] K. Y. Bliokh and F. Nori, Transverse spin and surface waves in acoustic metamaterials, Phys. Rev. B **99**, 020301(R) (2019).
[42] Y. Long, H. Ge, D. Zhang, X. Xu, J. Ren, M.-H. Lu, M. Bao, H. Chen, and Y.-F. Chen, Symmetry selective directionality in near-field acoustics, Natl. Sci. Rev. **7**, 1024 (2020).
[43] S. Wang, G. Zhang, X. Wang, Q. Tong, J. Li, and G. Ma, Spin-orbit interactions of transverse sound, Nat. Commun. **12**, 6125 (2021).
[44] C. Wan, J. Chen, A. Chong, and Q. Zhan, Photonic orbital angular momentum with controllable orientation, Natl. Sci. Rev. **9**, nwab149 (2021).
[45] M. V. Berry, Optical vortices evolving from helicoidal integer and fractional phase steps, J. Opt. A **6**, 259 (2004).
[46] M. V. Berry, R. G. Chambers, M. D. Large, C. Upstill, and J. C. Walmsley, Wavefront dislocations in the Aharonov-Bohm effect and its water wave analogue, Eur. J. Phys. **1**, 154 (1980).
[47] F. Vivanco, F. Melo, C. Coste, and F. Lund, Surface Wave Scattering by a Vertical Vortex and the Symmetry of the Aharonov-Bohm Wave Function, Phys. Rev. Lett. **83**, 1966 (1999).
[48] See Supplemental Material at http://link.aps.org/supplemental/10.1103/PhysRevLett.131.014001 for details of Laguerre-Gaussian spatiotemporal acoustic vortex beams, the experimental setup, transverse spreading effect at different moments, and Hilbert transform of the measured acoustic signals, which includes Refs. [49,50].
[49] M. Mazanov, D. Sugic, M. A. Alonso, F. Nori, and K. Y. Bliokh, Transverse shifts and time delays of spatiotemporal vortex pulses reflected and refracted at a planar interface, Nanophotonics **11**, 737 (2022).
[50] H. E. De Bree, The microflown: an acoustic particle velocity sensor, Acoust. Aust. **31**, 91 (2003).
[51] S. Huang, P. Wang, X. Shen, J. Liu, and R. Li, Diffraction properties of light with transverse orbital angular momentum, Optica **9**, 469 (2022).

[52] Z. Zou, R. Lirette, and L. Zhang, Orbital Angular Momentum Reversal and Asymmetry in Acoustic Vortex Beam Reflection, Phys. Rev. Lett. **125**, 074301 (2020).

[53] C. Wan, Q. Cao, J. Chen, A. Chong, and Q. Zhan, Toroidal vortices of light, Nat. Photonics **16**, 519 (2022).

[54] C. Wan, Y. Shen, A. Chong, and Q. Zhan, Scalar optical hopfions, eLight **2**, 22 (2022).

[55] M. Yessenov, L. A. Hall, K. L. Schepler, and A. F. Abouraddy, Space-time wave packets, Adv. Opt. Photonics **14**, 455 (2022).